Expansibility of vermiculite (Santa Luzia, Brazil) irradiated with microwave

F. M. N. Silva[1], T. R. B. Barros[1], T. S. B. Barbosa[1], E. G. Lima[1], T. L. A. Barbosa[1], M. G. F. Rodrigues[1]*
[1]Federal University of Campina Grande, Center of Sciences and Technology, Academic Unit of Chemical Engineering, R. Aprígio Veloso 882, 58429-970, Campina Grande, PB, Brazil

Abstract

The effect of microwave heating on the expansion of vermiculite was studied at a level of 700 W for 4 min exposure time and compared with raw vermiculite. In this study, the characterization of vermiculite from a mine in the northeast region of Brazil was performed using thermogravimetry, N_2-adsorption, cation exchange capacity, X-ray powder diffraction (XRD), infrared (IR) spectroscopy, X-ray fluorescence spectroscopy (XRF), and scanning electron microscopy (SEM). Following the microwave heating, the vermiculite was characterized using XRD, IR spectroscopy, and SEM. Microwave irradiation of the vermiculite sample caused structural changes such as loss of crystallinity and disorder, as revealed by the XRD patterns, but did not cause expansion. Results from SEM and IR spectroscopy showed that the microwave heating did not cause profound alterations to the morphology, clay structure, and chemical composition of the vermiculite.

Keywords: vermiculite, microwave heating, irradiation, expansibility.

INTRODUCTION

Clay minerals have significant commercial importance because they are cheap and relatively simple to process. Several areas of the industry have increased their interest in the clay minerals kaolinite, montmorillonite, and vermiculite [1]. Brazil has abundant reserves of vermiculite in several northeastern states (Piauí, Paraíba, and Bahia) as well as in Goiás. Vermiculite essentially consists of hydrated silicates of aluminum, iron, and magnesium and can be formed through the alteration of biotite [2]. Its structural formula can be represented by: $(Mg,Fe)_3[(Si,Al)_4O_{10}](OH)_2.4H_2O$ [3]. Microwave heating has rapidly become an effective tool in many different technological and scientific fields. Microwaves are part of the electromagnetic spectrum with wavelengths ranging from 1 m to 1 mm, corresponding to a frequency range from 300 MHz to 300 GHz. Unlike conventional heating, which works through heat transfer, microwave irradiation transforms electromagnetic energy into thermal energy. Microwave energy is applied directly to the material through molecular interaction with the electromagnetic field [4, 5]. Microwave sintering has achieved acceptance worldwide due to some significant advantages over conventional sintering methods. One of these advantages is that microwave sintering consumes much less energy than conventional sintering [6].

The performance of vermiculite in a given application depends highly on its thermal expansibility. Some exfoliation plants may use different furnace configurations, but the general sequence of operations is similar [7-9]. Vermiculite

can expand many times in volume when heated quickly, due to the sudden release of water between its layers [10, 11]. Expanded vermiculite has many desirable physical and chemical properties, such as low density, chemical stability, high cation exchange capacity, and high adsorption capacity [12], which make it useful for a variety of applications [13-18]. Expanded vermiculite can be prepared by three different methods: chemical expansion, microwave expansion, and high-temperature calcination expansion. In microwave expansion, molecular water is first penetrated by high-frequency microwaves, causing them to begin to vibrate and collide with each other to produce frictional heat, finally leading to expansion, when compared to the initial vermiculite size [19, 20]. The vermiculite expansion behavior is affected principally by the heating time and the microwave power [21]. Some studies have been carried out to investigate the performance of thermal expansion of vermiculite [22, 23]. It was found that further expansion was achieved with mixed-layer vermiculite minerals containing vermiculite in different hydration states [10].

There are only a few published articles on the microwave expansion of vermiculite to date. The influence of microwave power on vermiculite exfoliation characteristics, after treatment with water and hydrogen peroxide solution, was studied under experimental conditions of 600, 950, and 1300 W for microwave exposure times of 10, 20, 30, 60, 120, and 300 s [18]. The influence of microwave power on the expansion of vermiculites at 800 W for different exposure times (from 10 to 600 s) was investigated and compared with the changes from heating to 1000 °C and dehydration in a vacuum [20]. Ideal conditions were determined for exfoliation of raw vermiculite using microwaves and the performance of vermiculite in removing copper ions was evaluated [24]. When 100 g of crude vermiculite was

*meiry.rodrigues@ufcg.edu.br
https://orcid.org/0000-0003-2258-4230

irradiated at 440 W for 330 s, 66% of the crude vermiculite was exfoliated. Knowledge of vermiculite's dielectric properties, its interaction with electromagnetic fields, and materials technology were used to design and build a high-performance microwave system, operating at 2.45 GHz. The methodology used was reported [25]. Industrial samples of vermiculite from the Weili mine in Xinjiang province were expanded by chemical and chemical microwave methods and the expanded vermiculite mechanism was analyzed. As a result, vermiculite expands due to the oxygen pressure produced by the decomposition of hydrogen peroxide in the vermiculite interlayer. When using the chemical microwave method, the pressure of oxygen and water between layers leads to increased expanded times [26]. The LABNOV (New Materials Development Laboratory, UFCG, Brazil) research group has worked on the thermal treatment on clays with success [27-35]. As can be observed, there is a lack of studies in the literature regarding natural vermiculite clay being modified through microwave thermal expansion. The main objective of this study is therefore to analyze the mineral vermiculite, studying its characterization and its capacity to expand through microwave heating.

MATERIALS AND METHODS

Material: raw vermiculite clay (RAW-VER, União Brasileira de Mineração, Santa Luzia-PB, Brazil) was sieved with a N° 200 (0.074 mm) sieve, according to a Brazilian ABNT standard.

Expansion experiment by microwave heating (MW): the transformations undergone by the vermiculite subjected to microwave irradiation (CNNM18, Consul) at 700 W and exposure time of 4 min were studied. In a microwave oven, heating depends on the power of the oven and contents of the water, density, and sample quantity [21].

Characterization: the chemical composition of the samples was determined by X-ray fluorescence spectroscopy (XRF), following the method described elsewhere [36, 37] using an X-ray energy dispersive spectrophotometer (S2 Ranger, Bruker). Samples were characterized by X-ray diffraction using a diffractometer (XRD 6000m, Shimadzu) at 30 mA and 40 kV with CuKα radiation (λ=1.5418 Å) in the range of 3-20° 2θ, a step of 0.02°, and a count time of 1 s per step. Thermal behavior was studied by thermogravimetry (TG) using a thermal analyzer (TG/DTG 60H, Shimadzu) in the range of 30 to 1000 °C under pure nitrogen gas flow with a heating rate of 10 °C/min. The textural characteristics of the sample were investigated by isothermal gas adsorption/desorption of N_2 at 77 K (ASAP 2020, Micrometrics). The specific surface area was measured with an accelerated surface area and a porosimetry system by the BET method [38]. Fourier transform infrared spectroscopy (FTIR) was performed using a spectrophotometer (Cary 600, Agilent Technol.) in the wavenumber range from 4000 to 400 cm^{-1}, with a step of 500 cm^{-1}, and a resolution of 4 cm^{-1}. For this analysis, first, the sample was sieved with a Tyler 200 mesh (74 μm) sieve, then, 0.007 g of the sample was mixed with

0.1 g of KBr and pressed with 5 ton during 30 s to form a disc specimen. The microstructural analysis of expanded vermiculite was performed by scanning electron microscopy (SEM, SSX 550, Shimadzu) at a voltage of 15 kV. The cation exchange capacity (CEC) values of the samples were determined using ammonium acetate solution [39] and a nitrogen distiller (MA-036Plus, Marconi). The volume used for titration was then recorded (ASTM D7503-10) and CEC was calculated by:

$$CEC = \frac{M.f. \, V_{HCl} \cdot 100}{Ms} \qquad (A)$$

where M is the molar concentration of HCl (0.1 M), f is the conversion factor of the acid (=1), V_{HCl} is the volume of HCl used for titration (mL), and Ms is the mass of sample (g).

RESULTS AND DISCUSSION

Fig. 1 shows the thermogravimetry (TG) results for RAW-VER. The TG curve of clean natural vermiculite presented a profile similar to the curve obtained by another study [40], with a more pronounced mass loss in the range between 100 and 250 °C and a minor loss at approximately 850 °C, described as a characteristic of the formation of new phases in the material [40]. Data regarding mass loss in different temperature ranges are listed in Table I. Normally, three forms of water can be found in vermiculite interlayers: adsorbed water, hydrate water, and constitutional water. The mass losses at low temperatures were related to the adsorbed and interlayer water. According to the TG curve in Fig. 1 and Table I, three stages were identified for the RAW-VER sample as the temperature increased from 25 to 800 °C. The first stage occurred between 25 and 88 °C with a mass loss of 4.36%, which could be attributed to the removal of water molecules adsorbed on the vermiculite surface. Subsequently, the sample underwent a second dehydration process (hydrate water) between 88 and 154 °C. The mass loss of 1.03% in this stage was mainly attributed to the water
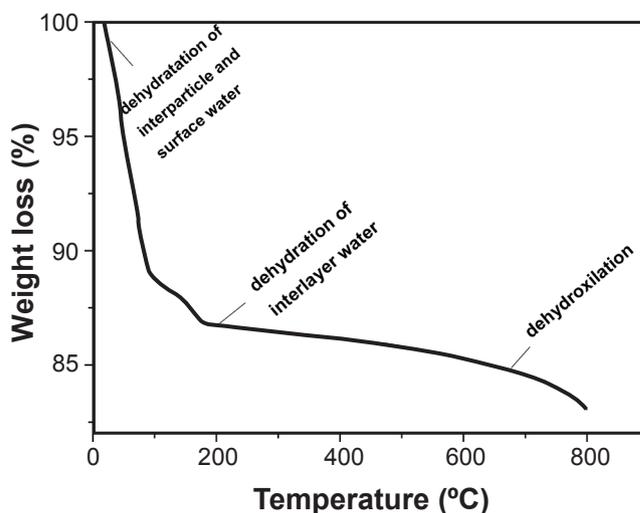
Figure 1: TG curve of the RAW-VER.

Table I - Mass loss (wt%) of RAW-VER at different temperature ranges.

<88 °C	88-154 °C	>500 °C	Total
4.36	1.03	1.79	7.18

bound to exchanged ions and dehydration of the RAW-VER. The third stage corresponded to the range from 154 to 838 °C with a mass loss of 1.79% (constitutional water) [40-43]. According to the literature [41], this mass change was mainly attributed to the removal of chemical structural water through a dehydroxylation reaction.

Nitrogen adsorption-desorption isotherm at liquid N_2 temperature for RAW-VER is shown in Fig. 2, while textural parameters of the sample are presented in Table II. According to Brunauer, the classification of the adsorption isotherm of RAW-VER is similar to type II [44]. With a hysteresis loop originating from the capillary condensation of liquid nitrogen in mesopores, the low-pressure region ($P/P_0 < 0.40$) represented the filling of micropores and the completion of the first monolayer on the external particle faces, which was followed by multilayer adsorption. In the relatively high-pressure region ($P/P_0 > 0.40$), the shape of the hysteresis loop corresponding to the filling of the mesopores was typical of type H3, where limiting adsorption took place at high P/P_0, which has been observed for aggregates of plate-like particles giving rise to slit-shaped pores. The specific surface area was determined by the BET and t-plot methods [38, 44-46], and the volumes of micro and mesopores in natural

clay are shown in Table II. The specific area of the RAW-VER sample was determined by the Brunauer, Emmett, and Teller (BET) method using nitrogen adsorption data from the relative equilibrium pressure interval of 0.05-0.35. The surface area of the RAW-VER sample was 38 m^2/g.

The cation exchange capacity (CEC) of clay minerals is defined as the quantity of cations available for exchange at a given pH expressed in meq/100 g which is equivalent to cmol(+)/kg [47, 48]. The CEC varies between 120 and 200 cmol(+)/kg for air-dried vermiculites and between 140 and 240 cmol(+)/kg for dehydrated vermiculites [49, 50]. The RAW-VER sample had a CEC value of 115 meq/100 g of clay, indicating that the clay contained a low amount of impurities or had a high isomorphic substitution level. Based on this premise, the value for the cationic exchange capacity is in agreement with the expected range for vermiculites.

The infrared spectra of RAW-VER and modified VER-MW are shown in Fig. 3. In Fig. 3a the 3750-2900 cm^{-1} range is characteristic of OH-stretching vibration, while bands located in the 1300-500 cm^{-1} range are the most informative about the structural characteristics of clay minerals and are attributed to lattice vibrations [51, 52]. The most important bands in the 3750-2900 cm^{-1} range for parent vermiculite are related to OH vibrations that have been perturbed by interlayer cations (3710 cm^{-1}) and unperturbed (3650 cm^{-1}) [53]. The most important bands found for raw vermiculite within the 1300-500 cm^{-1} range are related to stretching vibrations of Si-O-Si and Si-O in amorphous silica (at 1235 and 1075 cm^{-1}, respectively), stretching vibrations of Si-O in the clay layers (1165 and 995 cm^{-1}), stretching vibrations of Si-O and Al-O in the clay layers (weak band around 725 cm^{-1}), stretching vibrations of R-O-Si (where R= Al, Mg, or Fe; 675 cm^{-1}) and stretching vibrations of the OH group (weak band around 605 cm^{-1}) [54-59]. Microwave heating of RAW-VER resulted in a negligible modification of its IR spectra (Fig. 3b).

The results of chemical composition are shown in Table III. The presence of the following oxides was verified in vermiculite: SiO_2, MgO, Al_2O_3, Fe_2O_3, K_2O, P_2O_5, MnO, and

Figure 2: N_2 adsorption (filled square) and desorption (open square) isotherm of RAW-VER.

Table II - Textural parameters of RAW-VER.

S_{BET} (m^2/g)	R^2	Dp (nm)	S_{MI} (m^2/g)	S_E (m^2/g)	R^2	V_T (cm^3/g)
38	0.99996	5.625	7.01	30.79	0.99993	0.003

S_{BET}: surface area; S_{MI}: micropore area; S_E: external surface area; V_{MI}: micropore volume; V_T: total pore volume.
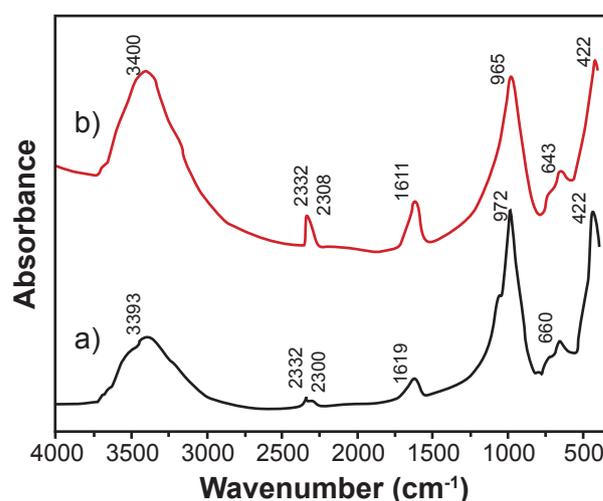
Figure 3: FTIR spectra of: a) RAW-VER; and b) VER-MW.

Table III - Chemical compositions (wt%) of RAW-VER and VER-MW determined by XRF analysis.

Sample	SiO_2	MgO	Al_2O_3	Fe_2O_3	K_2O	P_2O_5	MnO	TiO_2	CaO
RAW-VER	43.32	28.20	13.41	9.04	3.38	0.08	0.12	0.89	0.90
VER-MW	41.25	31.50	15.70	5.84	1.66	-	0.09	0.88	1.18

CaO. Silicon, magnesium, aluminum, and iron are the main components of vermiculite layers, while potassium, calcium, and possibly magnesium cations are located in the interlayer spaces within the clay. High content of MgO (28.20%) was observed. The values found for natural vermiculite were close to those of a vermiculite from China [41]. RAW-VER contained exchanged cations interlayered in distinct ionic layers, making them heterogeneous. The SiO_2, Al_2O_3, MgO, and Fe_2O_3 amounts were within the established ranges for most vermiculites of economic interest. Vermiculites generally show a wide variation in chemical composition, even within the same deposit or occurrence. This variation is due mainly to the differences in its mineralization, alteration of biotite mica, and degree of weathering [60]. Comparing

the composition of both samples, only slight differences were observed. The microwave heating did not significantly alter the composition of VER-MW [21, 22].

X-ray diffraction patterns of the RAW-VER and VER-MW vermiculite samples are presented in Fig. 4. The RAW-VER (Fig. 4a) showed broad peak reflection at 2θ=6.15° assigned to the (002) plane, showing the characteristic basal spacing d=1.438 nm, indicating a two-water layer hydration state [58-62], and this is a characteristic reflection for vermiculite (PDF file 00-034-0166). The characteristic peak of the VER-MW (Fig. 6b) may be found at 2θ=6.05° attributed to the (002) plane. The expansion was characterized by basal spacing corresponding to d=1.4609 nm, while the expansion that occurred using microwave was not effective as
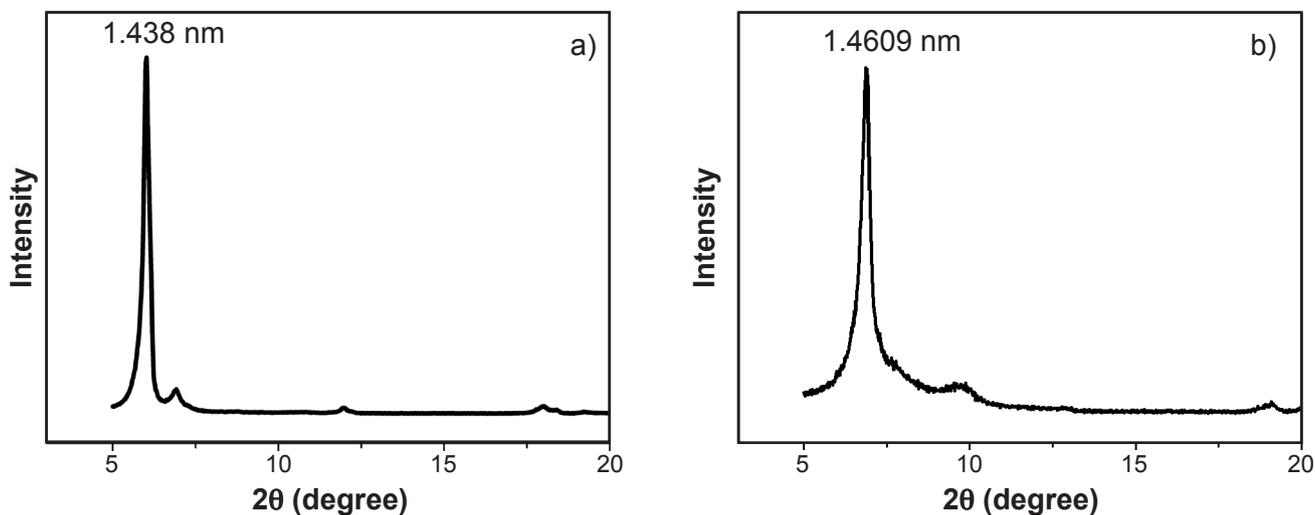
Figure 4: XRD patterns of vermiculite samples: a) RAW-VER; and b) VER-MW.
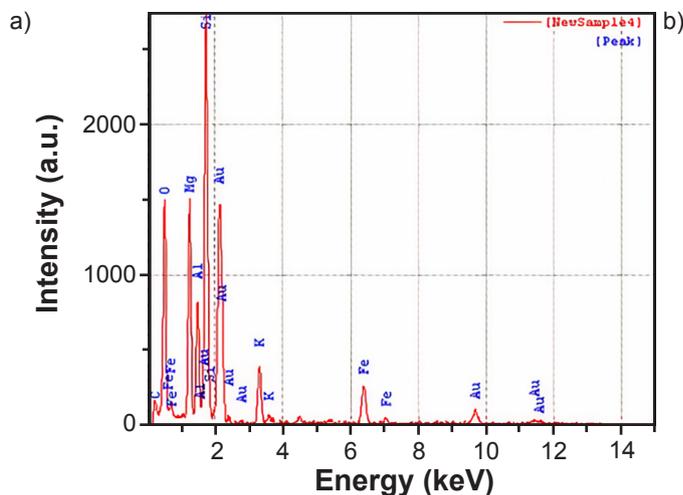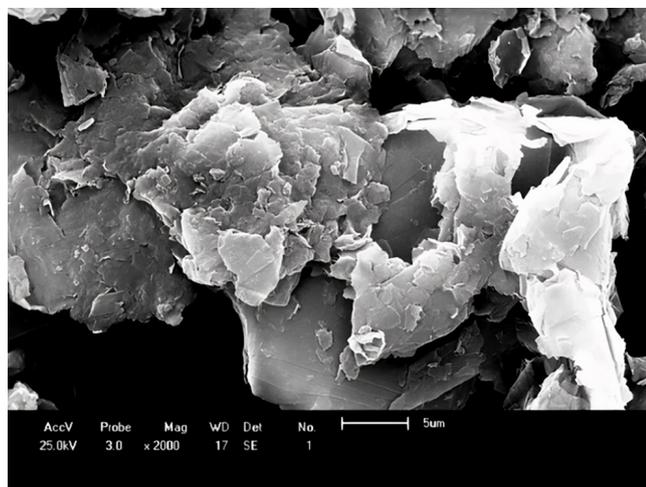
Figure 5: SEM image (a) and EDS spectrum (b) of RAW-VER.
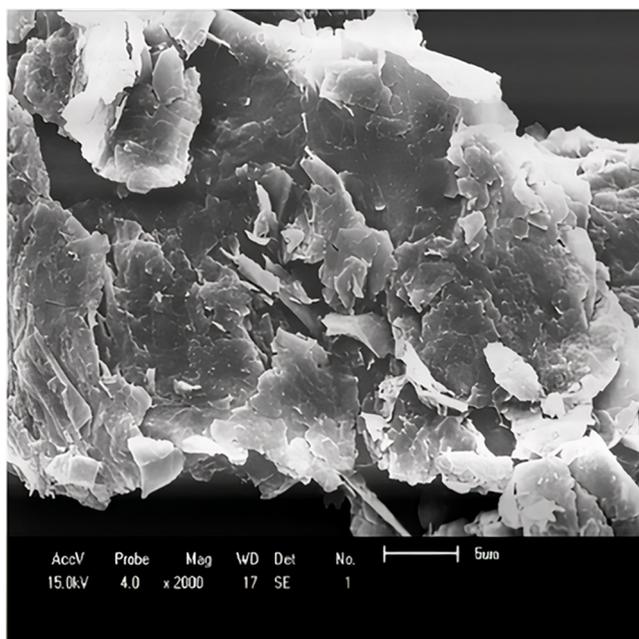
Figure 6: SEM image of VER-MW.

thermal expansion. From Fig. 4b, it can be seen that the intensity of the reflections of the VER-MW was reduced, indicating a reduction of crystallinity after heating. The expansion of the vermiculite particles depends on the irradiation time and the sample size. A possible explanation for the expansion of vermiculite not having occurred was the low microwave power. In this case, the microwave heating method showed that vermiculite still contained notable amounts of water. This was due to the complexity of the water-binding mechanisms in the clays.

Figs. 5 and 6 show SEM images revealing the morphologies of RAW-VER and VER-MW samples, respectively. RAW-VER (Fig. 5a) had a well-defined layered structure containing polygonal sheets with flaked borders with large vermiculite layer crystals. It was also observed a morphology with compact structure arranged in blocks of irregular shape [63, 64]. The energy dispersive spectroscopy (EDS) coupled to the SEM was used to determine the chemical elements present in the sample. RAW-VER sample (Fig. 5b) showed aluminum, magnesium, iron, and potassium. This result was in agreement with the results obtained by XRF (Table III). The expansion was related to the separation of the layers due to the water molecules release, which provoked significant changes in the morphology of the individual particles [22]. The micrograph of VER-MW (Fig. 6) showed irregular flakes of different sizes, and the presence of non-uniform aggregates and therefore without modification after heating by microwave treatment.

CONCLUSIONS

In this study, the expanded vermiculite (VER-MW) was prepared by the microwave heating method with a power of 700 W for 4 min. The microwave irradiation of the vermiculite caused structural changes, such as loss of crystallinity and disordering, as revealed by XRD patterns,

but did not cause the expansion process. It has been found that combined SEM, ED-XRF, and IR measurements are powerful tools for characterizing the vermiculite after the heating by microwave. Microwave heating caused no morphology, chemical composition, and structural changes in the sample as no major changes were observed in the SEM, ED-XRF, and IR analyzes.

REFERENCES

[1] P. Anadão, L.F. Sato, H. Wiebeck, F.R. Valenzuela-Díaz, Appl. Clay Sci. **48** (2010) 127.
[2] M. Alexandre, P. Dubois, Mater. Sci. Eng. **28** (2000) 1.
[3] M. Alexandre-Franco, A. Albarrán-Liso, V. Gómez-Serrano, Fuel Process. Technol. **92** (2011) 200.
[4] W. Wang, C. Zhao, J. Sun, X. Wang, X. Zhao, Y. Mao, X. Li, Z. Song, Energy **87** (2015) 678.
[5] J. Sun, W. Wang, Q. Yue, Materials **9** (2016) 231.
[6] M. Oghbaei, O. Mirzaee, J. Alloys Compd. **494** (2010) 175.
[7] A. Justo, C. Maqueda, J.L. Perez-Rodriguez, E. Morillo, Appl. Clay Sci. **4** (1989) 509.
[8] X. Huo, L. Wu, L. Liao, Z. Xia, L. Wang, Powder Technol. **224** (2012) 241.
[9] F. Bergaya, B.K.G. Theng, G. Lagaly (Eds.), "Handbook of clay science", Elsevier (2006).
[10] C. Marcos, I. Rodriguez, Appl. Clay Sci. **48** (2010) 492.
[11] H.F. Muiambo, W.W. Focke, M. Atanasova, I.V.D. Westhuizen, L.R. Tiedt, Appl. Clay Sci. **50** (2010) 51.
[12] U.G. da Silva Jr., M.A.F. Melo, A.F. da Silva, R.F. de Farias, J. Colloid Interface Sci. **260** (2003) 302.
[13] M.C. Jiménez De Haro, J.M. Martı́nez Blanes, J. Poyato, L.A. Pérez-Maqueda, A. Lerf, J.L. Pérez-Rodrı́guez, J. Phys. Chem. Solids **65** (2004) 435.
[14] G. Abate, L.B.O. dos Santos, S.M. Colombo, J.C. Masini, Appl. Clay Sci. **32** (2006) 261.
[15] O. Abollino, A. Giacomino, M. Malandrino, E. Mentasti, Appl. Clay Sci. **38** (2008) 227.
[16] M. Kehal, L. Reinert, L. Duclaux, Appl. Clay Sci. **48** (2010) 561.
[17] D. Mysore, T. Viraraghavan, Y.C. Jin, Water Res. **39** (2005) 2643.
[18] A. Gil, F.C.C. Assis, S. Albeniz, S.A. Korili, Chem. Eng. J. **168** (2011) 1032.
[19] A. Obut, I. Girgin, A. Yorukoglu, Clays Clay Miner. **51** (2003) 452.
[20] S.M. Sun, Y.S. Jiang, L.X. Yu, F.F. Li, Z.W. Yang, T.Y. Hou, D.Q. Hu, M.S. Xia, Mater. Chem. Phys. **98** (2006) 377.
[21] C. Marcos, I. Rodriguez, Appl. Clay Sci. **51** (2011) 33.
[22] Y. El Mouzdahir, A. Elmchaouri, R. Mahboub, A. Gil,

S.A. Korili, Powder Technol. **189** (2009) 2.

[23] E.M.M. Marwa, C.M. Rice, A.A. Meharg, Appl. Clay Sci. **43** (2016) 376.

[24] T. Lee, Environ. Technol. **32** (2011) 1195.

[25] O. Folorunso, C. Dodds, G. Dimitrakis, S. Kingman, Int. J. Miner. Process. **114-117** (2012) 69.

[26] Z. Miao, T.J. Peng, Y.G. Xi, W. Yang, Adv. Mater. Res. **96** (2010) 155.

[27] M.L.P. Silva, M.G.F. Rodrigues, M.G.C. Silva, Cerâmica **55**, 333 (2009) 11.

[28] W.C.T. Vilar, A.L.F. Brito, H.M. Laborde, M.G.F. Rodrigues, H.S. Ferreira, REMAP **4.3** (2009) 39.

[29] M.M. da Silva, A.C.L. Patrício, W.S. Lima, M.G.F. Rodrigues, H.M. Laborde, in 8th PTECH, Florianopolis (2011).

[30] P.N.M. Vasconcelos, "Modificação e caracterização de argila esmectita Brasgel visando seu uso no processo de remoção de metais pesados (Cd, Ni e Cd/Ni)", Doct. Thesis, UFCG, Campina Grande (2013).

[31] J.D. Mota, R.S.S. Cunha, M.G.F. Rodrigues, in 58th Congr. Bras. Cerâm., Bento Gonçalves (2014).

[32] W.S. Lima, A.L.F. de Brito, M.G.F. Rodrigues, M.F. Mota, M.M. Silva, Mater. Sci. Forum **805** (2015) 662.

[33] F.M.N. Silva, E.L. da Silva, I.F. dos Anjos, G. Fontgalland, M.G.F. Rodrigues, Mater. Sci. Forum **820** (2015) 36.

[34] T.R.B. Barbosa, T.S.B. Barbosa, M.G.F. Rodrigues, 4th CONAPESC, Campina Grande (2019).

[35] J.D. Mota, R.S.S. Cunha, P.N.M. Vasconcelos, M.G.F. Rodrigues, in "Princípios de química", C.L. Voigt (Org.), Atena Ed., Ponta Grossa (2019) 157.

[36] I. Barshad, F.M. Kishk, Contr. Mineral. Petrol. **24** (1969) 136.

[37] P.E. Mori, S. Reeves, C.T. Correia, M. Haukka, Rev. Bras. Geociênc. **29** (1999) 441.

[38] S. Brunauer, P.H. Emmett, E. Teller, J. Am. Chem. Soc. **60** (1938) 308.

[39] H.D. Chapman, in "Methods of soil analysis part 2: chemical and microbiological properties", C.A. Black, D.D. Evans, J.L. White, L.E. Ensminger, F.E. Clark, R.C. Dinauer (Eds.), Am. Soc. Agron., Madison (1965) 891.

[40] L.A. Pérez-Maqueda, V. Balek, J. Poyato, J.L. Pérez-Rodriquez, J. Šubrt, M. Bountsewa, N. Beckman, Z. Málek, J. Therm. Anal. Calorim. **71** (2003) 715.

[41] C. Marcos, Y.C. Arango, I. Rodriguez, Appl. Clay Sci. **42** (2009) 368.

[42] I. Barshad, Am. Mineral. **33** (1948) 655.

[43] J. Poyato, L.A. Pérez-Maqueda, A. Justo, V. Balek, Clays Clay Miner. **50** (2002) 791.

[44] J.C. Gregg, K.S.W. Sing, *Adsorption surface area and porosity*, Academic Press, London (1982).

[45] F. Rouquerol, J. Rouquerol, K. Sing, *Adsorption by powder and porous solids*, Academic Press, London (1999).

[46] S. Brunauer, L.S. Deming, D.M. Deming, E. Teller, J. Am. Chem. Soc. **62** (1940) 1723.

[47] P. Souza Santos, *Ciência e tecnologia de argilas*, 2nd ed., Edgard Blücher, S. Paulo (1992).

[48] F. Bergaya, M. Vayer, Appl. Clay Sci. **12** (1997) 275.

[49] J.A. Rausell-Colom, M. Fernández, J.M.J. Serratosa, F. Alcover, L. Gatineau, Clay Miner. **15** (1980) 37.

[50] C. de la Calle, H. Suquet, C.H. Pons, Clays Clay Miner. **36** (1980) 481.

[51] V.C. Farmer, Spectrochim. Acta **20** (1964) 1149.

[52] V.C. Farmer (Ed.), "The infrared spectra of minerals", 4, Mineral. Soc., London (1974).

[53] J. Madejová, Vib. Spectrosc. **31** (2003) 1.

[54] J.D. Russel, A.R. Fraser, in "Clay mineralogy: spectroscopic and chemical determinative methods", M.J. Wilson (Ed.), Springer, London (1994).

[55] D. Lin-Vien, N. Colthup, W. Fateley, J. Grasselli, *The handbook of infrared and Raman characteristic frequencies of organic molecules*, Academic Press, New York (1991).

[56] R.M. Silverstein, F.X. Webster, D.J. Kiemle, D.L. Bryce, *Spectrometric identification of organic compounds*, 8th ed., John Wiley Sons, New York (2005).

[57] J.R. Hidmam, in "Industrial minerals and rocks", 6th ed., D.D. Carr (Ed.), Soc. Min. Metal. Explor., Litleton (1994).

[58] M. Valášková, G.S. Martynková, A.M. Raaen, in "Clay minerals in nature: their characterization, modification and application", M. Valaskova (Ed.), Intech, London (2012).

[59] V. Medri, E. Papa, M. Mazzocchi, L. Laghi, M. Morganti, J. Francisconi, E. Landi. Mater. Des. **85** (2015) 266.

[60] L.N.F. de Queiroga, P.K. Soares, M.G. Fonseca, F.J.V.E. de Oliveira, Appl Clay Sci. **126** (2016) 113.

[61] C. Marcos, I. Rodríguez, Appl Clay Sci. **132-133** (2016) 685.

[62] D.G. Schulze, in "Soil mineralogy with environmental applications", J.B. Dixon, D.G. Schulze (Eds.), Soil Sci. Soc. Am., Madison (2002).

[63] X.-B. Yu, C.-H. Wei, L. Ke, H.-Z. Wu, Z.-S. Chai, Y. Hu, J. Colloid Interface Sci. **369** (2012) 344.

[64] Y. Zhang, Y. Gao, F. Yu, Q. Wang, Chem. Eng. J. **371** (2019) 424.